Dust-Storm Source Areas Determined by the Total Ozone Monitoring Spectrometer and Surface Observations

Richard Washington,* Martin Todd,** Nicholas J. Middleton,* and Andrew S. Goudie*

*School of Geography and the Environment, University of Oxford
**Department of Geography, University College London

Dust storms are recognized as having a very wide range of environmental impacts. Their geomorphological interest lies in the amount of deflation and wind erosion they indicate and their role in loess formation. Atmospheric mineral-dust loading is one of the largest uncertainties in global climate-change modeling and is known to have an important impact on the radiation budget and atmospheric instability. Major gaps remain in our understanding of the geomorphological context of terrestrial sources and the transport mechanisms responsible for the production and distribution of atmospheric dust, all of which are important in reducing uncertainties in the modeling of past and future climate. Using meteorological data from ground stations, from the space-borne Total Ozone Monitoring Spectrometer (TOMS), and from the National Center for Environmental Prediction–National Center for Atmospheric Research reanalysis project, we illustrate the key source regions of dust and demonstrate the primacy of the Sahara. Objectively defined source regions for the Sahara are determined from eigenvector techniques applied to the TOMS data. Other key regions include the Middle East, Taklamakan, southwest Asia, central Australia, the Etosha and Mkgadikgadi basins of southern Africa, the Salar de Uyuni (Bolivia), and the Great Basin (United States). In most of these regions, large basins of internal drainage, as defined from a digital elevation model, are dust sources where the near-surface atmospheric circulation (determined by calculated means of potential sand flux) is favorable for dust mobilization. Surface observations indicate some regions as being important that do not appear on the TOMS maps. Possible reasons for these discrepancies are explored. *Key Words: dust source areas, dust storms, TOMS.*

Dust storms cause a great variety of environmental impacts. Tropsopheric aerosols, including dust, are an important component of the earth's climate system and modify climate through their direct radiative effects of scattering and absorption (Tegen, Lacis, and Fung 1996), through indirect radiative effects via their influence on clouds microphysics (Rosenfeld, Considine, and Meade 1997), and by their role in processes of atmospheric chemistry (Schwartz, Wagener, and Nemesure 1995). Mineral dust in the atmosphere has terrestrial sources and represents an important process of land-atmosphere interaction. There has been considerable interest in analyzing surface observations of dust storms in the context of climate variability and change, and the human impact through land-use change (Goudie 1983; Middleton 1984, 1985, 1986a, 1986b, 1986c, 1991; Middleton, Goudie, and Wells 1986; Goudie and Middleton 1992). Indeed, Brooks and Legrand (2000) provide tentative evidence of a possible positive feedback mechanism involving rainfall and dust variability. Dust also has an impact on the nutrient dynamics and biogeochemical cycling of ecosystems, and it has a major influence on soil characteristics, oceanic productivity, and air chemistry. Moreover, because of the thousands of kilometers over which dust is transported, it has an influence at great distances from its sources (Goudie and Middleton 2001; Middleton and Goudie 2001).

Previous studies have used satellite observations to describe the large-scale dust-loading of the atmosphere over Africa (Brooks and Legrand 2000), the oceans (Husar, Prospero, and Stowe 1997), and globally (Herman et al. 1997). However, gaps remain in our understanding of the geomorphological context of terrestrial sources and the transport mechanisms responsible for the production and distribution of atmospheric dust. The importance of source regions of dust is underscored by the need for realistic inclusion of the dust cycle in climate models (Tegen et al. 2000). In this article, we investigate the large-scale structure of atmospheric dust and its relationship with the processes governing surface geomorphology and atmospheric circulation. Specifically, we:

- describe the mean global distribution of mineral dust;
- identify the key regions of deflational activity and the associated geomorphological context;
- assess the relative magnitude of various source areas; and
- consider the relationship of atmospheric dust and tropospheric transport mechanisms.

Annals of the Association of American Geographers, 93(2), 2003, pp. 297–313

Published by Blackwell Publishing, 350 Main Street, Malden, MA 02148, and 9600 Garsington Road, Oxford, OX4 2DQ, UK.

Data Sources

Owing to the recognition of the importance of atmospheric aerosol properties (Tegen, Lacis, and Fung 1996), interest in developing methods to retrieve such information from satellite data has increased. Satellites represent the only data source with truly global coverage and, in some cases, provide a record in excess of twenty years long. The signal measured by a satellite generally includes contributions from the earth's surface and the intervening atmosphere. Several methods have been developed to identify that signal related to the radiative effect of atmospheric aerosols, including single and multiple channel reflectance, multi-angle reflectance, contrast reduction, and polarization, as well as thermal infrared (TIR) emission (for a review, see King et al. 1999). Mineral dust from deserts and smoke plumes from volcanic eruptions and biomass burning have been observed by the increase in reflectance from the visible and infrared channels of the Advanced Very High Resolution Radiometer (AVHRR) sensor on board polar-orbiting National Oceanic and Atmospheric Administration (NOAA) satellites and the geostationary GOES and Meteosat satellites (Matson and Holben 1987; Holben, Eck, and Fraser 1991; Prinz and Menzel 1992; Moulin et al. 1997). Aerosol optical thickness and size distribution can also be retrieved from the multispectral visible and near infrared channels of the AVHRR (Durkee et al. 1991). Algorithms based on visible data are limited to oceanic regions, due to the need for a background surface with low and uniform reflectance. Legrand and colleagues (1989) describe a method in which estimates of dust are obtained from TIR data as a function of the observed suppression of upwelling thermal emission caused by a decrease in the short-wave surface radiative flux and, further, by long-wave absorption in the atmosphere. The effect of these processes is most pronounced over land surfaces. However, methods based on visible and infrared (IR) wavelengths suffer not only from a restriction to either ocean or land surfaces, but also from the effects of contamination by cloud (so that a cloud mask generally needs to be applied) and water vapor.

For this study, we employ the residue method of Herman and colleagues (1997), which uses observations in the ultraviolet (UV) from the Total Ozone Mapping Spectrometer (TOMS). This is based on multispectral measurements in the UV wavelengths and, in contrast to the techniques described above, allows detection of UV-absorbing aerosols over all surfaces due to the low and relatively uniform reflectivity of land and ocean surfaces. In addition, the method is unaffected by the presence of clouds. The TOMS sensor on board the Nimbus-7 satellite (launched in November 1978) is one of the most important satellite UV instruments. It is fortunate that the Nimbus-7 satellite operated continuously for 14.5 years, thereby providing a long-term database for study. The Nimbus-7 TOMS sensor has a spatial resolution of 100×100 km on average. These data have been remapped to a linear latitude/longitude projection and averaged to a resolution of 1×1.25 degrees (Herman et al. 1997). The raw data cover the period 1978 to 1993 and are available from the National Aeronautics and Space Administration (NASA) FTP site (ftp://jwocky.gsfc.nasa.gov/pub/nimbus7/data; last accessed in 2002, but still current in April 2003). Our work is based on the statistical analysis and mapping of these raw daily observations, which we define next.

Herman and colleagues' (1997) N-value residue method is based on the observed spectral contrast (the ratio of observed radiances) at 340 and 380 nm in relation to the spectral contrast as simulated by a modified version of Dave's (1978) LER model, in which it is assumed that the atmosphere consists only of molecular scatterers and absorbers and that the surface is bounded by a Lambertian surface. N-value residues (ΔN) are derived from

$$\Delta N = -100\{\log_{10}[I340/I380]_{obs} - \log_{10}[(I340/I380)_{calc}]\} \quad (1)$$

where the I_{obs} and I_{calc} are the backscattered radiances observed by satellite and simulated by the LER model, respectively. In order to distinguish clouds from absorbing aerosols, the method includes not only the change in spectral contrast relative to the "background" simulated radiances, but also the magnitude of the change. Radiative transfer calculations show that for a given change in I380, the spectral contrast depends strongly on the absorption optical thickness of the Mie scatterers, such that the contrast is highest for nonabsorbing aerosols/clouds and decreases with increasing absorption. UV-absorbing aerosols produce a smaller spectral contrast than predicted by the LER model and thus produce positive residues. The presence of clouds gives near zero residues, very similar to a simple increase in surface albedo. Radiative transfer simulations also show that nonabsorbing aerosols such as suspended sea salt and sulfate aerosols produce greater contrast and negative residues. Since we are interested here in the distribution of atmospheric dust, we restrict our analysis to positive residues of values greater than 0.7, since values below this may be contaminated by noise resulting from surface signal or nonabsorbing aerosols (Herman et al. 1997). Our aims, therefore, are consistent with the information content of the TOMS residues, in that we are concerned with understanding the mean structure of aerosol distribution at global and regional

scales in relation to geomorphological and atmospheric transport processes.

Other techniques have been developed using data from more recent and future satellite sensors that can provide more quantitative information on aerosol optical depth and properties—for example, the moderate resolution imaging spectroradiometer (MODIS) sensor on the NASA Terra satellite (King et al. 1999) and the observations from polarization and directionality of the earth's reflectances (POLDER) on board the advanced earth observing satellite (ADEOS) (Leroy et al. 1997). However, none of these provide data over the extensive time period necessary to identify the mean global structure of atmospheric dust provided by TOMS data.

In order to identify regions of dust production, we have calculated and mapped long-term means of TOMS aerosol index (AI) values from the raw daily AI values available from the NASA FTP site referenced above. In addition, we have calculated Varimax rotated empirical orthogonal functions (EOFs) of Saharan dust (over the domain 5°N – 36°N 20°W – 40°E) from the correlation matrix of TOMS monthly anomalies over the period of available record. To do this, we calculated the anomalies of the TOMS AI values whereby the long term mean of the K grid boxes (referred to now as variables) is removed from each respective grid box. Next, the correlation matrix, **[R]**, given by

$$\mathbf{[R]} = \mathbf{[D]}^{-1}\mathbf{[S]}\mathbf{[D]}^{-1} \qquad (2)$$

where **[D]** is the $(K \times K)$ diagonal matrix that has standard deviations of the K variables (here corresponding to the AI anomalies) computed. The matrix **[D]** consists of all zeros, except for the diagonal elements that have values that are the square roots of the corresponding elements of **[S]**. The correlation matrix **[R]** is the standardized equivalent of the variance-covariance matrix and indicates the degree of shared interannual variance between all the variables (here, grid boxes) in the domain.

EOF analysis is based here on the analysis of the correlation matrix **[R]**, so that **[R]** is simply a nondimensionalized version of **[S]**, the variance-covariance matrix, produced by dividing each element of **[S]** by the standard deviations of the variables in the *i*th row and *j*th column.

The EOFs are, in essence, new variables, u_m, that will account successively for the maximum amount of the joint variability of the data matrix found using the eigenvectors of **[R]**.

In this case, the EOFs we have calculated from the raw data will be used to indicate whether the source regions identified in the long-term mean are also spatially coherent regions with respect to interannual variability. EOFs of TOMS AI values have not been computed for other regions of global dust, since sensible EOFs will not emerge from these much smaller spatial domains.

In order to study the structure of the atmosphere associated with regions of high dust loadings, global analyses were obtained on a 2.5° grid from the National Center for Environmental Prediction (NCEP)–National Center for Atmospheric Research (NCAR) reanalysis project (Kalnay et al. 1996). Circulation data from several levels (surface, 850, 700, 500 and 200 hPa) were used in this study to represent surface, lower, middle, and upper tropospheric conditions, respectively. An evaluation of forecast products and circulation in the NCEP model can be found in Mo and Higgins (1996). The data source is henceforth referred to as "NCEP data."

In addition to studying the atmospheric circulation, we compute the potential sand transport in saltation, q, following White (1979) and Blumberg and Greeley (1996) as follows:

$$q = 2.61\, U_*^3\, p g^{-1}(1 - U_{*t}/U_*)(1 + U_{*t}/U_*)^2 \qquad (3)$$

where q = potential sand flux, g = acceleration due to gravity, p = fluid density, and U_{*t} = threshold shear stress (taken as a constant), with $U_{*;}$ = surface shear velocity given by

$$U_*^2 = \left(\tau_u^2 + \tau_v^2\right)^{0.5} p^{-1} \qquad (4)$$

where τ_u^2 and τ_v^2 are the surface zonal and meridional shear stress, respectively.

Sand transport potential is therefore a function of U_*^3, and the difference between the applied shear velocity and the threshold shear velocity. It was assumed that a constant threshold shear velocity exists over the surface of all areas and that the sand supply of all areas is unlimited. This is clearly violated in areas of bedrock or vegetation, for example, but we only interpret the quantity for source areas of dust derived from the TOMS data. The potential sand flux was computed from 6-hourly NCEP winds for twenty years of data (1980–1999) and averaged to make a long-term mean.

Finally, we used surface synops data of dust-storm events and visibility from Niger and Chad to illustrate the degree of agreement between TOMS AI data and traditional, surface-derived data. These were obtained for six stations—Tahoua, Zinder, Bilma, and Agadez in Niger and Faya and Ndjamena in Chad—following visits to these countries by the lead author.

The Global Picture

The world map of annual mean AI values determined by TOMS (Figure 1) has certain clear features. First, the largest area with high values is a zone that extends from

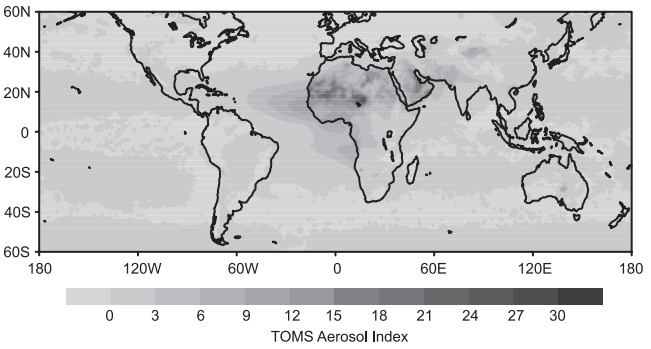

Figure 1. The world map of annual mean aerosol index (AI) values (× 10) determined by TOMS.

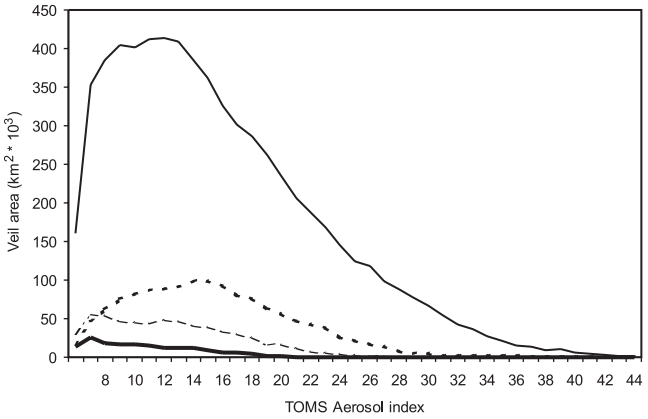

Figure 2. Area average TOMS aerosol index (AI) values for the main dust regions: Sahara, solid line; Arabia, heavy dashed line; Thar, light dashed line; northwest China, heavy solid line.

the eastern subtropical Atlantic through the Sahara Desert to Arabia and southwest Asia. In addition, there is a large zone with high AI values in central Asia, centered over the Tarim Basin and the Taklamakan Desert. Central Australia has a relatively small zone, located in the Lake Eyre basin, while southern Africa has two zones, one centered on the Mkgadikgadi basin in Botswana and the other on the Etosha Pan in Namibia. In Latin America, there is only one easily identifiable zone. This is in the Atacama and is in the vicinity of one of the great closed basins of the Altiplano. North America has only one very small zone with high values, located in the Great Basin.

The importance of these different dust "hot spots" can be gauged by looking not only at their areal extents, but also at their relative AI values. Table 1 lists the latter. This again brings out the very clear dominance of the Sahara in particular and of the Old World deserts in general. The southern hemisphere as a whole and the Americas are notable for their relatively low AI values. So, for example, the AI values of the Bodélé Depression of the south central Sahara are around four times greater than those recorded for either the Great Basin or the Salar de Uyuni in the Altiplano.

Table 1. Maximum Mean Aerosol Index (AI) Values for Major Global Dust Sources Determined from TOMS

Location	Mean AI Value
Bodélé Depression of south central Sahara	> 3.0
West Sahara in Mali and Mauritania	> 2.4
Arabia (southern Oman/Saudi border)	> 2.1
Eastern Sahara (Libya)	> 1.5
Southwest Asia (Makran coast)	> 1.2
Taklamakan/Tarim Basin	> 1.1
Etosha Pan (Namibia)	> 1.1
Lake Eyre Basin (Australia)	> 1.1
Mkgadikgadi Basin (Botswana)	> 0.8
Salar de Uyuni (Bolivia)	> 0.7
Great Basin of the United States	> 0.5

However, the best way to assess the relative importance of dust source areas on a global basis is to combine their areas and their AI values (Figure 2). This again brings out the enormity of the Saharan dust source in comparison with Arabia, China, and the Thar.

Dust Storms in the Sahara

The Sahara and its margins have long been recognized as the major source of aeolian soil dust in the world, with an annual production of 400–700 Tg per year (Schutz, Jaenicke, and Pietrek 1981; D'Almeida 1987; Swap, Garstang, and Greco 1992). However, within the Saharan context, there has been considerable debate as to the locations of the main dust-producing areas (Herman et al. 1999; Middleton and Goudie 2001). This has been caused in part by the absence of suitable surface-based observations over extensive areas. Some progress has been made in identifying source areas for dust by measurements of infrared radiances such as those acquired by METEOSAT. These can be used to produce the Infrared Difference Dust Index (IDDI) (Brooks and Legrand 2000). This method has highlighted the Bodélé Depression between Tibesti and Lake Chad as an important source, together with a large swathe covering portions of Mauritania, Mali, and southern Algeria. It also suggests that the Horn of Africa and the Nubian Desert in southern Egypt and northern Sudan are important sources. Kalu (1979) and Herman and colleagues (1999) have also shown the importance of the Bodélé, but the status of the other regions is less clear.

The TOMS data (Figure 3) confirm that the Bodélé is the most intense source, not only in the Sahara, but also in the world, with AI values that exceed 3.0. It also demonstrates the presence of a large but less intense area

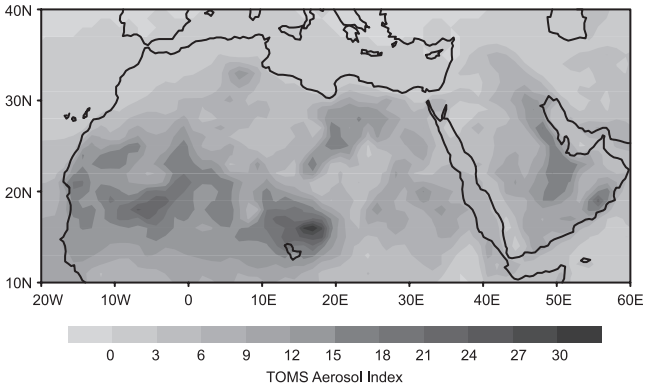

Figure 3. Annual average TOMS aerosol index (AI) values (×10) for the Sahara.

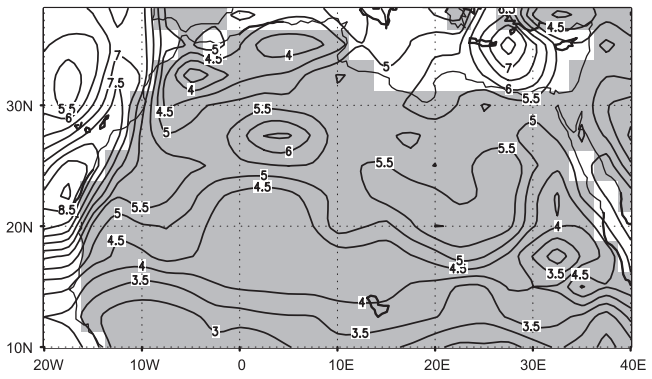

Figure 4. Long-term mean NCEP July–September surface wind speeds (m.s $^{-1}$) over the Sahara study domain. Shaded area is land as represented in the NCEP climate model.

(AI values over 2.4) in the west Sahara. This extends to the coast of Mauritania. Relatively high AI values can also be observed in the interior of Libya.

Varimax rotated EOFs of the annual TOMS AI anomalies identify the Bodélé as the leading EOF, once the first unrotated EOF relating to Saharan-wide dust has been removed. Spatially coherent, lower-order rotated EOFs also emerge for Mauritania, Mali, and southern Algeria (as one coherent EOF), the salt lakes of Tunisia, and northeast Algeria. Taken together, this suggests that the regions that emerge as having spatially coherent, long-term, mean annual AI values are also objectively identifiable as regions that behave similarly with respect to interannual variability. It is therefore reasonable to have identified these regions as core dust-producing areas on the basis of mean annual AI values alone.

The importance of the Bodélé as a source is a product of various factors. It is fed with alluvium by streams draining from the Tibesti, and there may also be susceptible silty materials that were laid down in an expanded Lake Chad during Holocene and Pleistocene pluvials. Moreover, Mainguet and Chemin (1990) have argued that deflational activity downwind from Tibesti may help to explain the excavation of Lake Chad itself.

The reasons for the importance of the west Saharan dust source in Mali, Mauritania, and Algeria are less well understood. However, it is an area of low relief bounded on the north and east by uplands. While such upland areas are not themselves major dust-source regions, wadis draining from them will have transported silt-rich alluvium into the area. Likewise, in the past, the southern part of the region may have received alluvium from the Niger prior to its capture by southeast-trending drainage near Tosaye (Urvoy 1942). It also contains an enormous closed depression some 900 km long and various ergs that could provide a dust source through winnowing. The depression contains many ancient lakebeds that show signs of intense Holocene deflation (Petit-Maire 1991). Dubief (1953) maps it as an area of high aeolian activity. It is also dry, with annual precipitation levels of 5–100 mm. Desiccation and sediment supply need to be accompanied by winds that are strong enough to mobilize material. The nature of the wind field is analyzed next.

Figure 4 shows the long-term, mean boreal summer (July–September) surface-wind speeds calculated from the NCEP–NCAR reanalysis project data (Kalnay et al. 1996) dataset over the Saharan study domain. This period corresponds with the season of highest AI values. Although average wind speeds are less than 5 m.s $^{-1}$ across the regions showing heaviest dust-loadings, values in excess of 5 m.s $^{-1}$ occur in a prominent zone along the Libyan–Chad border. The dust region corresponds very closely with a maximum in near-surface convergence (Figure 5), suggesting that convection is an important process initiating dust storms in this region. Dust transport from this source area is effected in an easterly jet apparent at the 850-hPa (approximately 1.5 km) level between 20 and 25° north (Figure 6), evidenced by the large negative u-component (i.e., easterly) winds. Taking the difference between the near-surface (850-hPa or approximately 1.5-km) zonal winds for the three most dusty summers (July to August) over the Bodélé in the data period studied (1991, 1984, and 1988) and subtracting the two summers with the lowest dust values (1981 and 1980) yields a clear signal pointing to the origin of the transport mechanism of dust, namely an anomalous easterly jet covering a broad area of the Sahara including North Sudan, Chad, and Niger, as well as South Egypt and Libya (Figure 7). It is clear that extremes in dust events are associated with atmospheric circulation changes on the scale of the general circulation.

Figure 8 shows an overlay of TOMS values, potential sand flux (q), and elevation derived from a digital

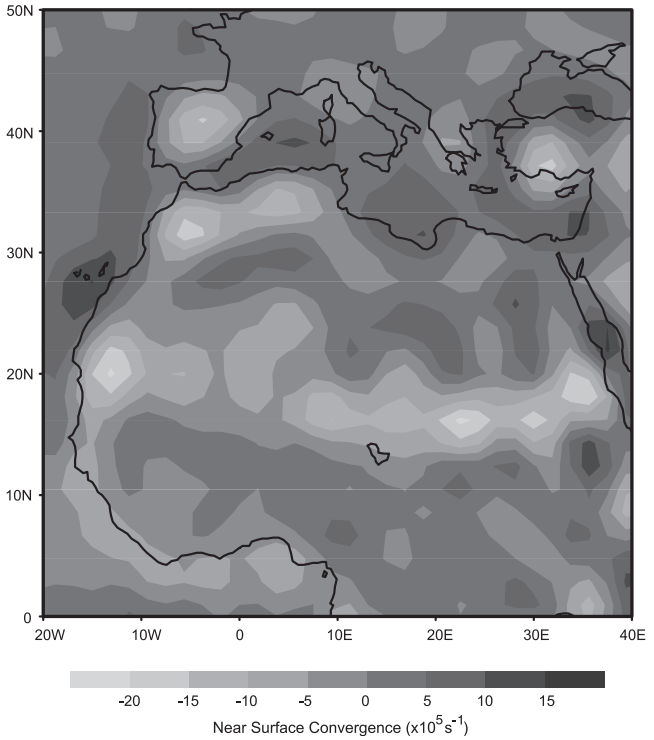

Figure 5. Long-term mean NCEP July–September near-surface divergence ($\times 10^6$ s^{-1}) over the Sahara study domain.

elevation model at 0.5° resolution. Data for TOMS AI values and for potential sand flux relate to the April to June season. Many of the features discussed earlier in this section are apparent. Most noticeable is the coincidence of the maxima in AI values over the Bodélé and the large values of potential sand flux. The Bodélé also lies immediately west of the regional maximum in sand-flux potential. Reasons for the high values of the latter are

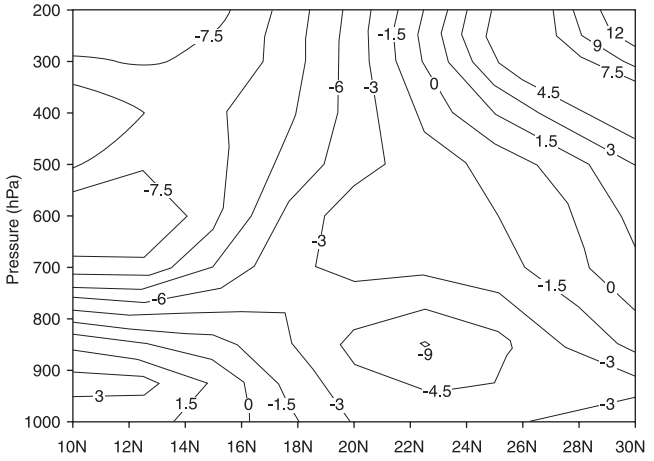

Figure 6. Latitude-height section of NCEP July–September long-term mean zonal (west to east) wind vectors (m.s^{-1}). The vertical axis is pressure. The section has been averaged over 20–30° E.

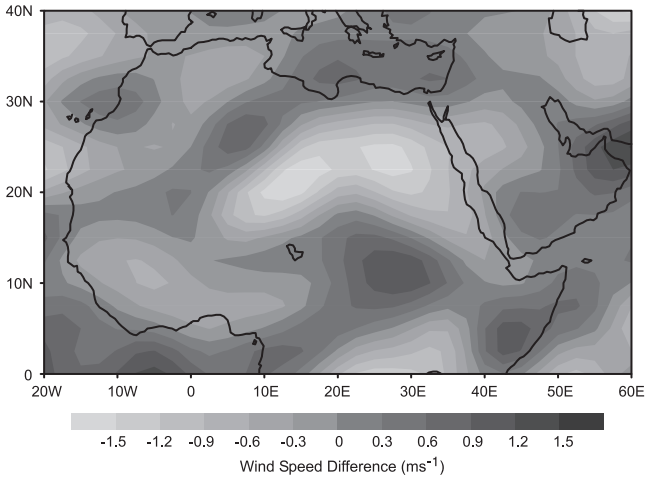

Figure 7. April to June zonal 850-hPa (approximately 1.5-km) wind speed differences (m.s^{-1}) between three years of extremely high dust content (1991, 1984, 1988) and two years of extremely low dust content (1981, 1980).

apparent in the elevation that points to the channeling of the wind to the south of the Tibesti. It is remarkable that the NCEP winds capture this feature so well, given the reasonably coarse resolution of the model. Interestingly, the dust maximum in Mali is also coincident with very high values of potential sand flux (even higher than to the east of the Bodélé AI maximum) and with an elevation minimum. In the case of Mali, though, the high values of potential sand-flux cover a larger area and may not be as topographically concentrated during individual events as they are in the case of the Bodélé. In the Sahara, a clear case can be made for (1) defining source regions from TOMS data, (2) explaining the origin of sediment supplied to the source regions, and (3) accounting for

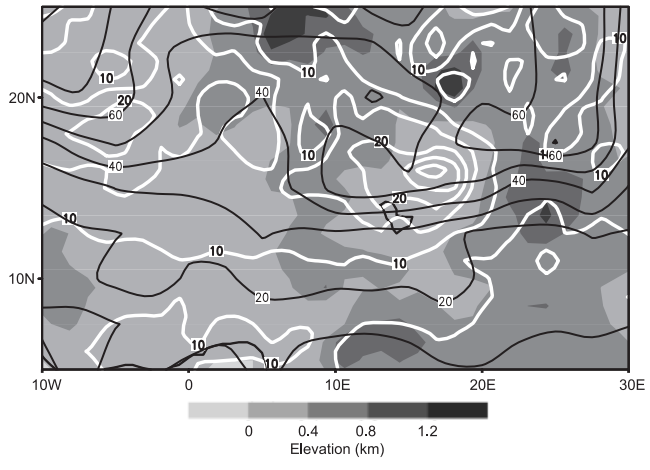

Figure 8. TOMS aerosol index (AI) values ×10 (white contours, contour interval 5), scaled potential sand flux (black contours, contour interval 10), and elevation in km (shaded) for the Sahara, long-term means, April–June.

the long-term mean and variability of the wind region associated with the dust main source regions.

Dust Storms in the Middle East

Middleton (1986a) has reviewed the distribution of dust storms in the Middle East. In addition, Idso (1976) recognized Arabia as one of five world regions where dust storm generation is especially intense. Prospero and Carlson (1981) reports that a major zone of dust haze can be observed in the Arabian Sea during June, July, and August, and high levels of dust have been found off the Omani coast (Tindale and Pease 1999). Pease, Tchakerian, and Tindale (1998) suggest that the Wahiba Sands could be a major dust source. Although there are severe gaps in terms of the coverage by surface stations with dust-storm observations—not least over the Rub Al Khali—Middleton (1986a) demonstrated that the Lower Mesopotamian plains had the highest number of dust-storm days per year. Central Saudi Arabia had a moderate level of dust storm activity, with Riyadh recording an average of 7.6 dust storm days per year, and 76 days on average when blowing dust reduced visibility to less than 11 km.

The TOMS data (Figure 3), indicate that the Middle East is an important area of dust-storm activity, but rather than highlighting the Lower Mesopotamian Plains as a source region, it shows the importance of the Ad Dahna erg region of eastern and central Saudi Arabia. It also shows a small area of intense dust-storm activity with AI values greater than 2.1 in the Saudi-Oman border region. This is the third most intense dust source that TOMS indicates in the world. It is an area of intense aridity fed by ephemeral rivers draining from the mountains of Yemen and Oman. The NCEP-NCAR reanalysis data shows the mean July to September seasonal winds (corresponding to the months of highest dust loadings in the TOMS data) to be light across Saudi Arabia, although with moderately higher winds on the coastal margins (not shown). A more thorough study of individual dust-storm events would be necessary to confirm the hypotheses that (dry) convection, occurring at the mesoscale, is an important mechanism for generating dust in this region. Such studies are restricted by access to wind data at an appropriately fine resolution. In contrast, the large-scale Asian Monsoon inflow, which is well resolved in datasets such as the NCEP–NCAR reanalysis, reaches a maximum off the coast of Oman, with the center of the low level jet in excess of 16 m.s $^{-1}$. In all probability, the secondary maximum in dust loadings found over Oman relates to the concentration of the Monsoon inflow along the topography of Oman.

Dust Storms in Southwest Asia

The swathe of desert that stretches from Iran through Afghanistan and Pakistan into northwest India has long been recognized as a source of atmospheric soil dust (Bryson and Baerreis 1967; Grigoryev and Kondratyev 1981). Dust storms have received considerable attention in India (see, e.g., Joseph 1982; Negi et al. 1996) and Middleton (1986b) has prepared a regional dust climatology. Dust from desert sources in southwest Asia provides a significant contribution to aerosols over the Arabian Sea (Chester, Berry, and Murphy 1991; Tindale and Pease 1999) and to its deep-sea sediments (Sirocko 1991; Bloemendal et al. 1993).

Multiple dust sources are discernible on the annual mean map of TOMS data (Figure 1 and Figure 9). These sources are broadly concurrent with those mapped by Middleton (1986b) using data observed at meteorological stations (Figure 10). Figure 9 shows four major source areas with AI values of >0.8: the Makran coastal zone, stretching from southeastern Iran into neighboring Pakistan; a broad area of central Pakistan; an area at the convergence of the borders of Iran, Afghanistan, and Pakistan that comprises the Seistan Basin, Registan,

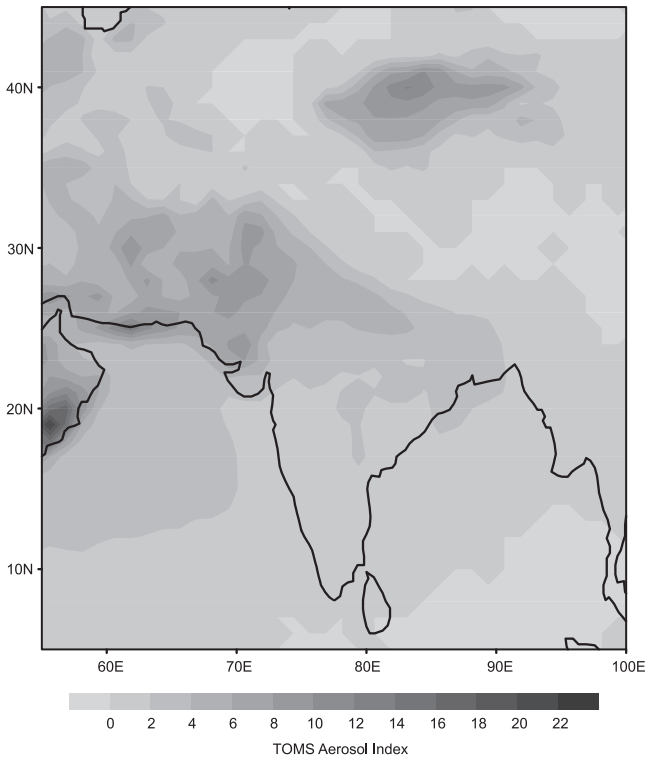

Figure 9. Annual average TOMS aerosol index (AI) values ($\times 10$) for southwest Asia.

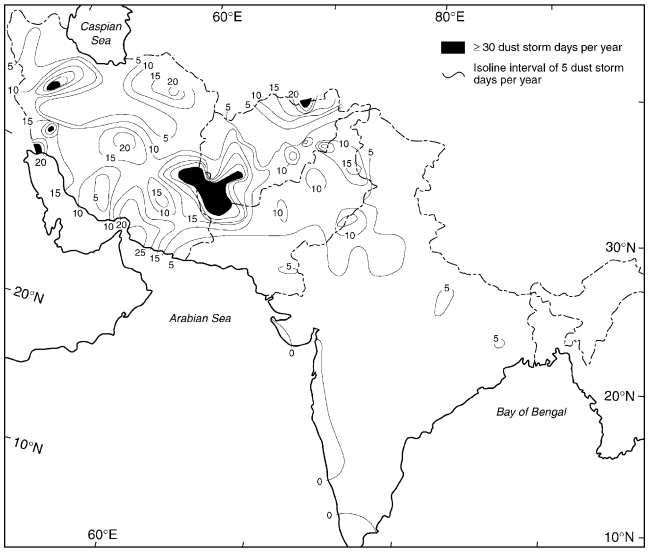

Figure 10. Distribution of surface-observed dust-storm frequencies in southwest Asia. Source: after Middleton (1986a).

and northwestern Baluchistan; and an area approximately coincident with the Indus delta. A broad "tongue" of dust-raising activity stretching southwestward down the alluvium of the Gangetic plain is also clearly defined on both maps.

Coastal Baluchistan/Makran appears as the most active source area according to the TOMS data, whereas Middleton's (1986a) map (Figure 10) shows the Seistan Basin area to have the most frequent dust-storm activity. Middleton does not record the Indus Delta as a significant area for dust-storm activity, having fewer than five dust storms a year. However, Middleton highlights the plains of Afghan Turkestan as an area where annual dust-storm frequency exceeds thirty and two areas in Iran (around Yazd in the center and along the border with Turkmenistan) as having twenty or more dust storm days annually. None of these areas appears significant according to the TOMS data.

The Makran is a hyperarid area of late-Quaternary uplift (Vita-Finzi 1981; Reyss et al. 1998). Material is supplied to the coastal strip from the mountains inland, and silt-sized material blown from ephemeral rivers and alluvial fans southward over the Arabian Sea dominates near-shore sediments (Mohsin, Farooqui, and Danish 1989). The Iran/Afghanistan/Pakistan border area is known as the Dasht-i-Margo. Dust sources are found in lowland parts of this mountainous region, including the Seistan Basin. Sediments available for deflation are fed into the basin from the surrounding mountains. Specific source areas are likely to be alluvial fans and ephemeral lakes.

Dust Storms in China

Dust storms take on particular importance in China because of their significance for the formation of loess (Derbyshire, Meng, and Kemp 1998). They also appear to have been a major source of the dust in Late Pleistocene ice layers in Greenland (Svensson, Biscaye, and Grousset 2000). Moreover, according to Kes and Fedorovich (1976), the Tarim Basin has more dust storms than any other location on Earth, with 100–174 per year. There are stations to the northwest of the 750-mm annual rainfall isohyet that have dust storms on more than thirty days in the year (Goudie 1983). They can cover immense areas and transport particles to Japan and beyond (Ing 1969; Willis, Easterbrook, and Stephenson 1980; Betzer et al. 1988). They are also frequent in Mongolia (Middleton 1991), most notably in the southern region of the Gobi, where Zamiin Uud has over 34 dust storms per year.

Studies of dust loadings (Chen, Fryear, and Yang 1999) and fluxes have suggested that there are two main source areas: the Taklamakan and the Badain Juran (Zhang et al. 1998). In all, it has been estimated that about 800 Tg of Chinese dust is injected into the atmosphere annually, which may be as much as half of the global production of dust (Zhang, Arimoto, and An 1997).

Figure 11 shows the best available map of dust storms in the region. The predominant importance of the Taklamakan (which includes the Tarim Basin) is evident, though other important centers occur north of Urumqi in the Junggar Pendi and in the Ordos.

The TOMS data (Figure 12) confirm the primacy of the Taklamakan/Tarim source. A large area stretching from

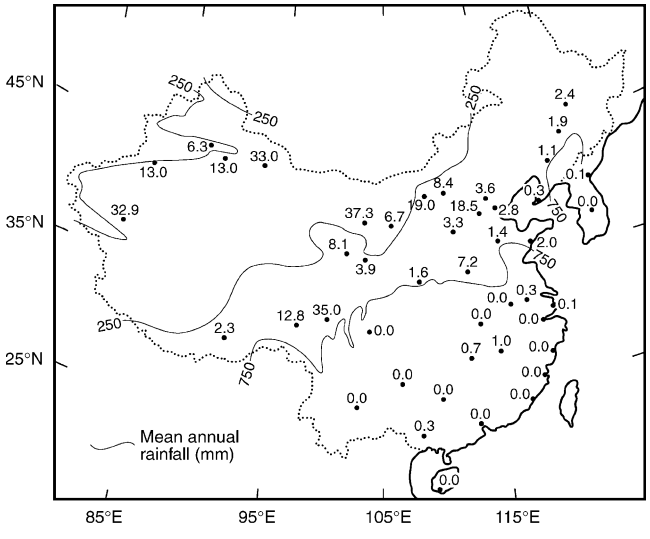

Figure 11. Distribution of surface-observed dust-storm frequencies in China. Source: after Derbyshire, Meng, and Kemp (1998).

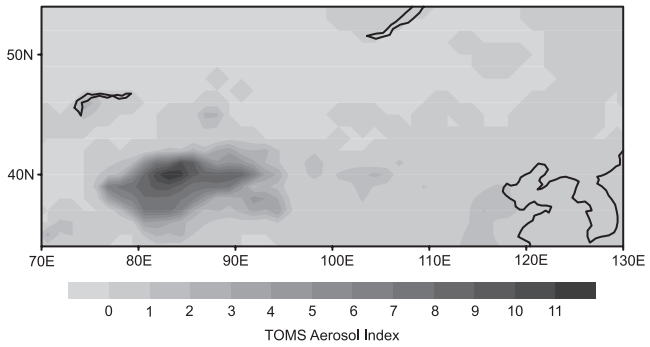

Figure 12. Annual average TOMS aerosol index (AI) values (×10) for China.

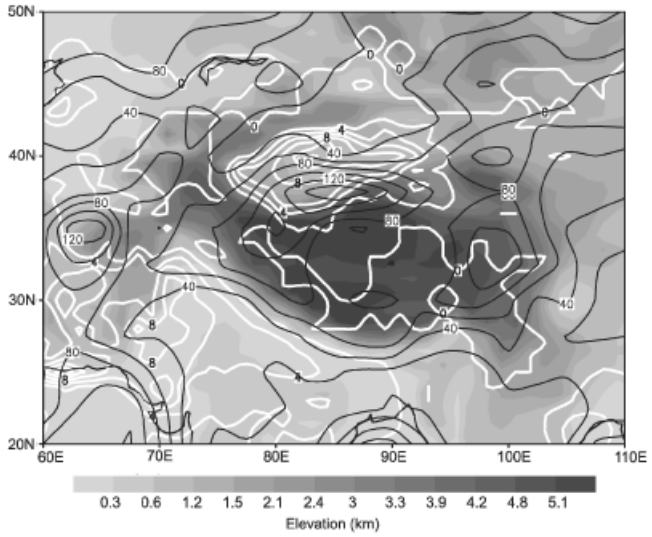

Figure 13. TOMS aerosol index (AI) values ×10 (white contours, contour interval 2), scaled potential sand flux (black contours, contour interval 20) and elevation in km (grey scale) for China, long-term annual means.

75–94°E and from 35–42°N has relatively high AI values, which exceed 1.1 in the center. The Junggar Pendi shows up as a secondary source, as do some small areas to the east of the Taklamakan towards Beijing. The TOMS mean values are in broad agreement with modeled dust production (Xuan, Gualiang, and Du 2000), in that both show an east-to-west increase in dust, with a primary peak in the Tarim and a spring maximum. However Xuan, Gualiang, and Du (2000) suggest a secondary peak over West Mongolia, which is not evident in the TOMS data. These disparities are discussed in more detail at the end of this article.

The primacy of the Taklamakan as a source is scarcely surprising. It is the largest desert in China, has a precipitation that can drop to less than 10 mm, and consists of a closed basin into which mountain rivers feed sediments. There are extensive marginal fans, areas of dune sand from which dust can be winnowed (Zhu 1984; Wang and Dong 1994; Honda and Shimuzu 1998) and lake sediments associated with the wandering and desiccated lake of Lop Nor. Above all, with an area of 530,000 km^2, the Tarim is one of the earth's largest closed basins. However, the TOMS data do not indicate that it is a source of similar magnitude to northern Africa. The area with high AI values is both smaller and less intense.

The atmospheric circulation associated with dust of Asian origin has been the subject of numerous studies (see, e.g., Iwasaka, Minoura, and Nagaya 1983; Littman 1991; Zaizen et al. 1995; Husar et al. 1999) and is known to be enhanced during the boreal spring (Prospero and Savoie 1989; Jaffe et al. 1997; Talbot et al. 1997, Husar et al. 1999). The circulation over the Taklamakan is highly complex, owing to the influence of the seasonally reversing monsoon and the extreme bounding topography, thereby obstructing throughflow of the prevailing winds. Dust-loadings are highest in the late winter and spring and are probably associated with cold waves or surges of the NE monsoon. Given the complexity of the terrain, low-level airflow is a tough test of a coarse-resolution model such as NCEP. The model does, however, show a local maximum in surface-wind velocity (not shown) at the southern edge of the Taklamakan, presumably where the cold-air advance is blocked. An additional explanation could be that the dust-laden atmosphere is poorly ventilated, so that dust products remain trapped in the enclosed basin.

Figure 13 shows an overlay of TOMS values, potential sand flux (q) and an elevation derived from a digital elevation model at 0.5° resolution. Data for TOMS AI values and for potential sand flux relate to the annual mean. The largest potential sand-flux values in the entire domain (20–50°N, 80–110°E) are in very close proximity to the maximum in AI values. The highest potential sand-flux values are only slightly offset to the south of the AI values and run up against the Tibetan plateau. As in the case of the Bodélé, high potential sand-flux values relate to regions of extreme topographic channeling of the winds. In this case, the channeling occurs through one of the largest closed basins in the world.

Dust Storms in the Southern Hemisphere

Southern Africa is not a major area of dust production, but it has a large area of arid terrain both in the coastal Namib and in the interior (Kalahari and Karoo). There are many pans (Goudie and Wells 1995), which are at least in part the result of deflation, and there are wind-streaks and yardangs in the Namib. Satellite images show dust plumes blowing westwards towards the South Atlantic (Eckardt, Washington, and Wilkinson 2002). In addition, there are loess and loess-like deposits (Blumel 1991).

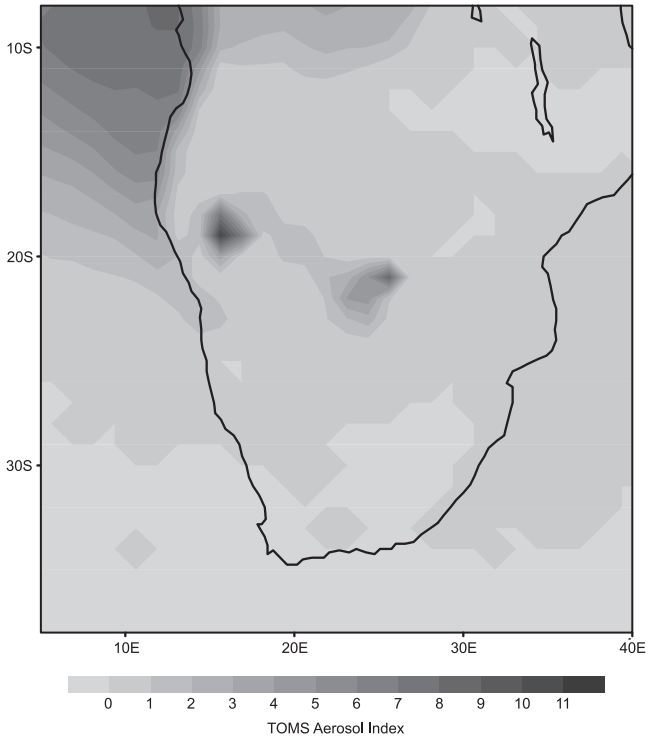

Figure 14. Annual average TOMS aerosol index (AI) values (×10) for southern Africa.

The TOMS analyses (Figure 14) indicate two relatively small but clearly developed dust sources. The more intense of these is centered over the Etosha Pan in northern Namibia and has an AI value of more than 1.1. The other center is over the Mgkadikgadi Depression in northern Botswana and has AI values greater than 0.8.

Etosha, which covers an area of about 6,000 km^2, comprises a salt lake that occupies the sump of a much larger basin and often floods in the summer months. For the most part, it is dry enough in winter for deflation to occur, as is shown by extensive lunette dunes on its lee side (Buch and Zoller 1992). It is fed by a system of ephemeral channels—*oshanas*—that have laid down large tracts of fine-grained alluvial and lacustrine sediments. In the past, it may have received inputs of material from the highlands of Angola via the Cunene (Wellington 1938). The coexistence of fluvial inputs and of a structural depression means that the Etosha Basin contains the greatest thickness of Kalahari beds in the whole of the Kalahari (Thomas and Shaw 1991).

The Mkgadikgadi is another major structural feature, the floor of which is now occupied by a series of saline sumps. Sua (Sowa) Pan has an area of around 3,000 km^2. In wet years floods occur, but in most years the combined extents of the salt pans is considerable. They then present surfaces from which deflation can and does occur. The pans are, however, but remnants of a pluvial lake, Lake Palaeo-Mkgadikgadi, which at its greatest extent was over 50 m deep and covered 120,000 km^2. It was second in Africa only to pluvial Lake Chad. It was fed with water and sediment from the Okavango and, perhaps, Zambezi systems, and by more locally derived rivers flowing from the south—the now dry *mekgacha* of the Central Kalahari (Nash, Thomas, and Shaw 1994).

Dust events in the southern African source regions are invariably associated with enhancement of the low-level easterly circulation over the interior (Eckardt, Washington, and Wilkinson 2002). Transient eddies, in the form of west-to-east migrating anticyclones traveling to the west of a Rossby wave-trough axis, are confined to the oceanic areas immediately to the south of the subcontinent as a result of the unbroken escarpment (de Wet 1979; Tyson and Preston-Whyte 2000). The migration of mass in these systems leads to an enhanced east-west gradient and the corresponding anomalous easterlies, which, over the western half of the subcontinent, are associated with dust storms and plumes over the subtropical southeast Atlantic.

Figure 15 shows an overlay of TOMS values, potential sand flux (q) and an elevation derived from a digital elevation model at 0.5° resolution. Data for TOMS

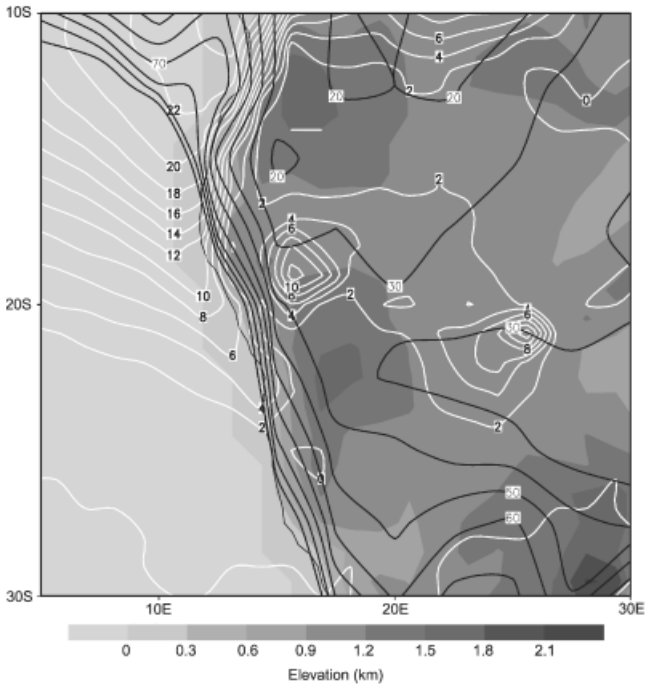

Figure 15. TOMS aerosol index (AI) values ×10 (white contours, contour interval 2), scaled potential sand flux (black contours, contour interval 10) and elevation in km (shaded) for southern African, long-term means, July–September.

AI values and for potential sand flux relate to the July–September season, which corresponds with the season of largest AI values in the Etosha and Mkgadikgadi pans. Unlike the cases of the AI maxima in the Sahara and China, there is no clear association between a maximum of potential sand flux and AI values. Neither of the two pans is located in a region where topographic channeling of the wind would accelerate it sufficiently to produce a large dust source. Instead, it is likely that the southern Africa dust sources are supply-limited, with suitable material available only from the two pans.

Aeolian processes are of considerable importance in Australian deserts, as evidenced by sand dunes (Wasson et al. 1988) and extensive deposits of aeolian clay (*parna*) (Dare-Edwards 1984). However, although almost three-quarters are a dryland, the continent's deserts produce relatively small amounts of dust. Nonetheless, this has received considerable recent attention (Middleton 1984; McTainsh, Burgess, and Pitblado 1989; Nickling, McTainsh, and Leys 1999), and the area of greatest dust-storm frequency, as determined from meteorological station data, has been shown to be broadly coincident with the huge (1.3 million km^2) internal drainage basin of Lake Eyre. Indeed, the TOMS analysis indicates that this ephemeral playa is the continent's main dust source, the only area where AI values exceed 1.1. The dustiness of the current playa bed itself can only be inferred from terrestrial data, due to the absence of meteorological stations.

As an area of sediment supply, the Lake Eyre Basin has been compared to that of Lake Chad (McTainsh 1985), with deflation operating on alluvial spreads brought by the southward flowing Eyre, Diamantina, and Cooper Rivers. The long history of deflation is evidenced by wind-blown deposits, typically rich in gypsum and clay, found at a number of sites (Magee and Miller 1998).

Throughout the months of maximum atmospheric dust-loadings (October to March) the surface-wind speeds reach a maximum over the Simpson and Great Victorian deserts (apart from the west coast of Australia), with a prevailing southeasterly to southerly wind (not shown). The classic synoptic situation generating deflation in southern regions of Australia is an eastward moving mid-latitude frontal system (Sprigg 1982). Anticyclogenesis may follow the passage of the front, producing marked horizontal wind shear in the easterlies to the south of a heat trough (Sturman and Tapper 1996). Material raised by these systems is occasionally transported as far as New Zealand (Collyer et al. 1984).

Information on the occurrence of dust storms in South America is sparse. However, Johnson (1976) suggests that they are a feature in the Altiplano of Peru, Bolivia, and Chile. Middleton (1986c) has mapped the occurrence of dust events in Argentina and noted their importance on the Puna de Atacama, where salt basins—*salars*—appear to be an important source. The presence of closed depressions and of wind-fluted topography, combined with the probable importance of salt-weathering in the preparation of fine material for deflation (Goudie and Wells 1995), suggest that the dry areas of the Altiplano should indeed be major source areas for dust. The TOMS-derived map (not shown) identifies one area in South America where AI values are relatively high (i.e., greater than 0.7; see Table 1). This appears to be centered on the Salar de Uyuni, a closed basin in the Bolivian Altiplano, which lies astride 20° S latitude and is located in an area with 200 to 400 mm of annual rainfall. This salar, the largest within the Andes, is possibly the world's largest salt flat, though in the Late Pleistocene it was the site of the huge pluvial Lake Tauca (Lavenu, Fournier, and Sebrier 1984; Clayton and Clapperton 1997). It is bounded by high shorelines and impressive algal incrustations (Rouchy et al. 1996) and is more than 600 km long. It is possible that the sediments from its desiccated floor are one of the reasons for the existence of high AI values in this region. It is of the same order of size as some of the other basins that are major dust sources (e.g., the Bodélé/Chad, Eyre, Tarim, and Mkgadikgadi).

Dust Sources in North America

North America is a classic area for dust-storm studies, not least because of the severe dust-bowl years of the 1930s (Worster 1979). Human pressures on the land surface have led to severe dust episodes since then (Wilshire, Nakata, and Hallet 1981; Gill 1996). Details of dust generation have been provided in a number of regions, including the Owens Lake of California (Reheis 1997), the Mojave and Colorado deserts (Bach, Brazel, and Lancaster 1996), and North Dakota (Todhunter and Cihacelik 1999). Reheis and Kihl (1995) provide a study of dust deposition for Nevada and California. Surface weather station observations have tended to suggest that for the United States as a whole, the greatest frequency of dust events occurs in the panhandles of Texas and Oklahoma, Western Kansas, Eastern Colorado, the Red River Valley of North Dakota, and Northern Montana. These areas combine erodible materials with a dry climate, and, most importantly, high values for wind energy (Orgill and Sehmel 1976; Changery 1983; Gillette and Hanson 1989) (Figure 16).

The TOMS data (not shown) give a rather different picture, and show only one area with maximum AI values greater than 0.5—parts of the Great Basin. This is an area of fault-bounded blocks and troughs. It contains over 150

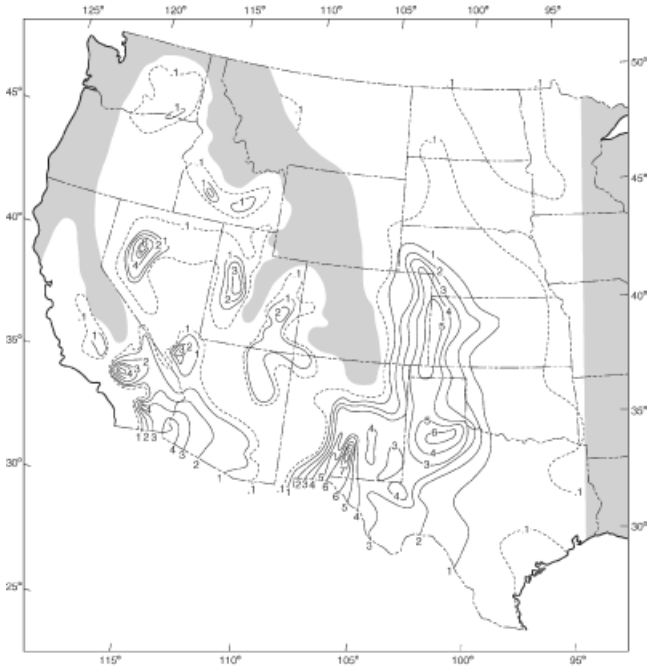

Figure 16. Distribution of surface-observed annual dust-storm frequency in the United States. Shaded areas represent no observations of dust storms. Source: after Orgill and Sehmel (1976).

basins separated from each other by north-south trending mountain ranges. Most of the basins were occupied by Pleistocene lakes that covered an area at least eleven times greater than the area they cover today (Grayson 1993, 86). One of these was Bonneville, which was roughly the size of present-day Lake Michigan. Another was Lahontan, which covered an area roughly as great as present-day Lake Erie. Their desiccation, the presence of extensive areas of salty lake floor (Blank, Young, and Allen 1999), and the existence of large expanses of alluvial fans running into the many basins may account for the importance of this area as a dust source.

Disparities between Surface-Based TOMS AI Data

Although the TOMS data appear to provide a picture of the main dust-source areas that coincides with those determined from surface observations, there are some areas that TOMS does not identify as being major sources. This is true of parts of the United States, Kuwait and Iraq, certain parts of the former Soviet Union, and Mongolia's Gobi Desert. In the case of the United States, the Great Plains do not emerge as a major source, whereas the Great Basin does. Similarly, although Kuwait has a comparable number of dust storm days to the Bodélé, it (Middleton, Goudie, and Wells 1986; Table 1) and its neighborhood do not emerge as being of great importance in the TOMS analyses. In the former Soviet Union, there are many stations that have in excess of forty dust-storm days per year (Klimenko and Moskaleva 1979), and dust evacuation from the desiccating floor of the Aral Sea is a major environmental problem. The Gobi Desert in southern Mongolia has been noted for its high dust-storm frequency (Middleton 1991) and as a source area for trans-Pacific transport (Husar, Husar, and Martin 2000).

There are two possible kinds of explanations for the anomalous situation in the Great Plains. On the one hand, much of the dust may occur at low levels and so may not be detected by TOMS. Three synoptic patterns are associated with dust events in the southern High Plains (Wigner and Peterson 1987). One of these is convective modification of the boundary layer. This accounts for 42 percent of dust events at Lubbock and causes strong winds at low levels, particularly in late morning (Lee et al. 1994). Another 19 percent of all events are caused by thunderstorm outflows, which again may have a limited vertical extent. The passage of cold fronts accounts for a further 30 percent of dust events in Lubbock, but the relatively stable cold air behind the fronts usually limits the vertical spread of dust. In addition, while the map of dust-storm occurrence in the United States is based on the work of Orgill and Sehmel (1976), the TOMS data relate to an entirely different and more recent period. Over that time, changes in land use have caused a decrease in dust-storm activity in some areas, including Lubbock (Ervin and Lee 1994) and North Dakota (Todhunter and Cihecek 1999).

In the case of China, several potential reasons for the differences between surface- and satellite-based observations evident in Figures 11 and 12. These include:

1. A different period of coverage, which would be important in multi-annual variability of the atmospheric circulation/rainfall and/or land-use, as is the case for the Great Plains.
2. Differences deriving from the interpolation of the surface data points, since we cannot be sure that surface observations in the region of the TOMS maximum are also not very high, as the former are sparsely distributed. For example, there is only one observation in the Tarim basin (32.9 storms per year), whilst in the Gobi region the values are highly variable (3.9–37.3).
3. The fact that surface synops reports and TOMS are not measuring the same phenomenon. The former are binary, while the latter relates to optical thickness on a linear scale.

Accepting that there is a disparity between the surface observations and TOMS, a number of possible reasons exist why the AI signal over the Gobi desert may be biased. These include:

1. mineralogy, which has a large affect on the optical properties of dust particles. In radiative transfer simulations of the effect of aerosols on UV radiances, Torres and colleagues (1998) used estimates of the complex refractive index of dust based on observations of Sahara dust. This may not be appropriate to the Gobi.
2. the well-known difficulties TOMS has with sampling the boundary layer, which may be compounded by the anomalously strong subsidence into the Taklamakan.
3. dust mixing with sulfates (non-absorbing aerosol) over West China, resulting in lower residuals because sulfates scatter both upwelling and downwelling UV.

The Sahara is one region where surface-based observations are in good qualitative agreement with the TOMS AI data. In order to explore this relationship more quantitatively, visibility data from surface stations in Niger and Chad were correlated with the TOMS AI data. Figure 17 shows the correlations between Bilma visibility data for 1980–1993 and the TOMS AI data over the domain 20°S–40°N, 50°W–50°E. Bilma lies at the eastern edge of the Tenere desert and is the closest synops station downwind of the Bodélé. The correlations have been calculated for four seasons (January to March, April to June [AMJ], July to September, and October to December [OND]), but Figure 17 shows only two of these (AMJ and OND). During the season of peak dust emission from the Bodélé (AMJ), the correlations between surface visibility and TOMS AI values are strong and large in scale. Peak correlations in this season occur some distance downwind of Bilma, pointing to an offset between the surface-based data and TOMS, which probably relates to the fact that TOMS samples the depth of the atmosphere rather than the near surface. The remaining seasons, exemplified by October–December in Figure 17, show generally poor agreement both locally and regionally between the surface-based and remotely sensed data. Again, it is likely that the atmospheric circulation is doing much to cause these differences, in that dust is likely to be transported in complex ways in the near-surface layers. It is clear that the quantitative relationship between TOMS and surface-based data is an extremely complex issue and one that cannot be addressed in full in this exploratory article.

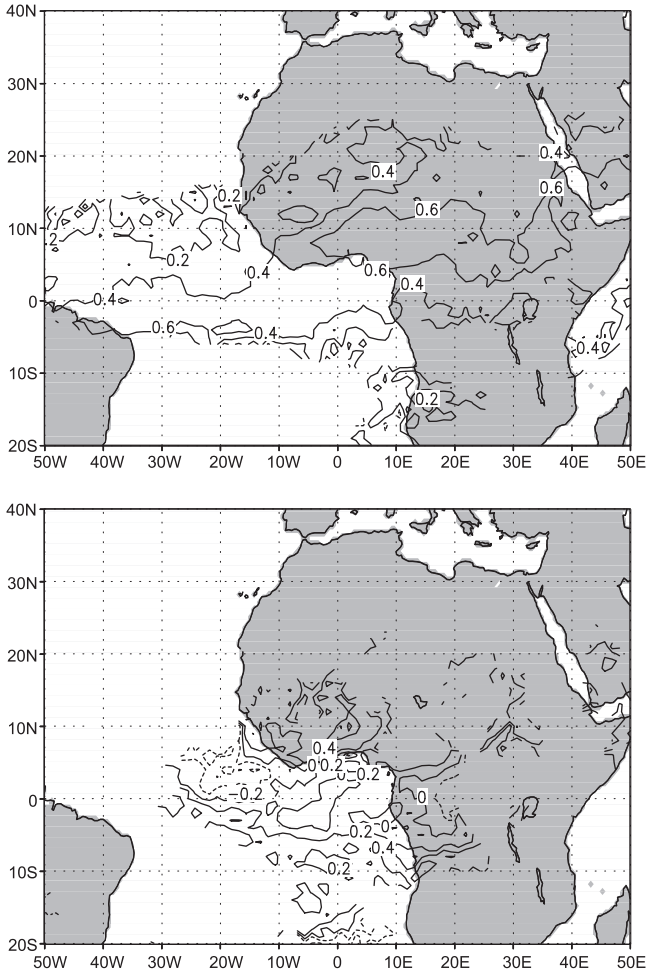

Figure 17. Correlations between surface synops visibility data (1980–1993) for Bilma, Niger, and TOMS aerosol index (AI) values for April–June (top) and October–December (bottom). Broken contours indicate locations where too few nonzero TOMS aerosol index (AI) values have been recorded to make correlation meaningful.

Conclusion

Analysis of TOMS data has enabled a global picture of desert dust sources to be determined. It has demonstrated the primacy of the Sahara, and has also highlighted the importance of some other parts of the world's drylands, including the Middle East, Taklamakan, southwest Asia, central Australia, the Etosha and Mkgadikgadi of southern Africa, the Salar de Uyuni in Bolivia, and the Great Basin in the United States. One characteristic that emerges for most of these regions is the importance of large basins of in-ternal drainage as dust sources (the Bodélé, Taoudenni, Tarim, Eyre, Etosha, Mkgadikgadi, Etosha, Uyuni, and the Great Salt Lake). Our findings are in excellent agreement with the recent independent analysis of Prospero and colleagues (2002).

Eigenvector-based analysis of the correlation matrix of TOMS data for the Saharan domain indicates that basins identified in the Saharan region are objectively identifiable from the perspective of interannual variability as well. This independent method of objectively defining the key dust regions justifies the simple approach taken in the rest of this article—namely, the description of the long-term mean AI values.

Analysis of the NCEP circulation data reveals the ability of a coarse-resolution climate model to capture some of the main controls on dust production. In particular, the calculation of potential sand flux (q) from surface NCEP winds reveals a remarkable coincidence of peak q values in association with peak AI values, particularly where the near-surface circulation is topographically channeled (the latter having been assessed by means of a digital elevation model).

However, there are some regions indicated by surface observations as being important that do not appear as such on the TOMS maps, including the Kuwait region and parts of the United States and the former Soviet Union. The reasons for such discrepancies need more investigation. In nearly all regions important to dust generation, features of the near-surface atmospheric circulation likely to be associated with dust events are discernible in the NCEP reanalysis dataset. In the cases of China and southern Africa, topography plays an important part in modifying the flow associated with midlatitude transients. In the Sahara, the enhancement of the planetary scale near surface easterly jet appears to be closely associated with extreme dust events. Future work will use trajectory modeling to identify more precisely the production and transport of dust and to examine in much greater detail whether discrepancies between surface- and satellite-derived products derive from the nature of near-surface circulation.

Acknowledgments

The authors would like to express their gratitude to Mathew J. Swann for help with computing and graphics and to Ailsa Allen for drafting some of the figures.

References

Bach, A. J., A. J. Brazel, and N. Lancaster. 1996. Temporal and spatial aspects of blowing dust in the Mojave and Colorado deserts of southern California, 1973–1994. *Physical Geography* 17:329–53.

Betzer, P. R., K. L. Carder, R. A. Duce, J. T. Merrill, N. W. Tindale, M. Uematsu, D. K. Costello, R. W. Young, R. A. Feely, J. A. Breland, R. E. Bernstein, and A. M. Greco. 1988. Long-range transport of giant mineral aerosol-particles. *Nature* 336 (6199): 568–71.

Blank, R. R., J. A. Young, and F. L. Allen. 1999. Aeolian dust in a saline playa environment, Nevada, USA. *Journal of Arid Environments* 41:365–81.

Bloemendal, J., J. W. King, A. Hunt, P. B. Demenocal, and A. Hayashida. 1993. Origin of the sedimentary magnetic record at Ocean Drilling Program Sites on the Owen Ridge, western Arabian Sea. *Journal of Geophysical Research* 98 (B3): 4199–219.

Blumberg, D. G., and R. Greeley. 1996. A comparison of General Circulation Model predictions to sand drift and dune orientations. *Journal of Climate* 9:3248–59.

Blumel, W. D. 1991. Kalkrusten—Ihre genetischen Bexiehungen zu Bodenbildung und aolischer Sedimentation (Calcrete: Genetic relationship to soil formation and Aeolian sedimentation). *Geomethodica* (Basel) 16:169–97.

Brooks, N., and M. Legrand. 2000. Dust variability and rainfall in the Sahel. In *Linking climate change to land-surface change*, ed. S. McLaren and D. Kniveton, 1–25. Dordrecht: Kluwer Academic Publishers.

Bryson, R. A., and D. A. Baerreis. 1967. Possibilities of major climatic modification and their implications, Northwest India: A case for study. *American Meteorological Society Bulletin* 48:136–42.

Buch, M. W., and L. Zoller. 1992. Pedostratigraphy and thermoluminescence-chronology of the western margin- (Lunette-) dunes of Etosha Pan, Northern Namibia. *Wurzburger Geographische Arbeit* 84:361–84.

Changery, M. J. 1983. *A dust climatology of the western United States*. National Ocean and Atmospheric Administration ID NOAA_C00016. Prepared by the National Climatic Data Centre/National Environmental Satellite, Data, and Information Service for the U.S. Nuclear Regulatory Commission. Asheville, NC: National Climatic Data Centre.

Chen, W., D. W. Fryear, and Z. Yang. 1999. Dust fall in the Takla Makan Desert of China. *Physical Geography* 20: 189–224.

Chester, R., A. S. Berry, and K. J. T. Murphy. 1991. The distributions of particulate atmospheric trace metals and mineral aerosols over the Indian Ocean. *Marine Chemistry* 34:261–90.

Clayton, J. D., and C. M. Clapperton. 1997. Broad synchrony of a late-glacial advance and the highstand of palaeolake Tauca in the Bolivian Altiplano. *Journal of Quaternary Science* 12:169–82.

Collyer, F. X., B. G. Barnes, G. J. Churchman, T. S. Clarkson, and J. T. Steiner. 1984. Trans-Tasman dust transport event. *Weather and Climate* 4:42–46.

D'Almeida, G. A. 1987. Desert aerosol characteristics and effects on climate. In *Paleoclimatology and paleometeorology: Modern and past patterns of global atmospheric transport*, ed. M. Leinen and M. Sarthein, 311–38. Dordrecht: Kluwer.

Dare-Edwards, A. J. 1984. Aeolian clay deposits of southeastern Australia: Parna or loessic clay? *Transactions of the Institute of British Geographers* 9:337–44.

Dave, J. V. 1978. Effect of aerosols on the estimation of total ozone in an atmospheric column from the measurement of its ultraviolet radiation. *Journal of Atmospheric Science* 35: 899–911.

Derbyshire, E., X. Meng, and R. A. Kemp. 1998. Provenance, transport, and characteristics of modern aeolian dust in western Gansu Province, China, and interpretation of the

Quaternary loess record. *Journal of Arid Environments* 39:497–516.

de Wet, L. W. 1979. Die invloed van die Suid-Afrikaanse hoogland op die ontwikkeling en voortplanting van atmosferiese druk en sirkulasiestelsels (The influence of the South African highveld on the development and propagation of atmospheric pressure and circulation systems). Master's thesis, Department of Meteorology, University of Pretoria.

Dubief, J. 1953. La vent et la deplacement du sable du Sahara (Wind and the displacement of the sand of the Sahara). *Travaux de L'Institut de Recherches Sahariennes* 8:123–64.

Durkee, P. A., F. Pfeil, E. Frost, and R. Shema. 1991. Global analysis of aerosol particle characteristics. *AtmosphericEnvironment* 25A:2457–71.

Eckardt, F., R. Washington, and M. J. Wilkinson. 2002. The origin of dust on the west coast of southern Africa. *Palaeoecology of Africa and the Surrounding Islands* 27:207–19.

Ervin, R. J., and J. A. Lee. 1994. Impact of conservation practices on airborne dust in the southern High Plains of Texas. *Journal of Soil and Water Conservation* 49:430–37.

Gill, T. E. 1996. Eolian sediments generated by anthropogenic disturbance of playas: Human impacts on the geomorphic system and geomorphic impacts on the human system. *Geomorphology* 17:207–28.

Gillette, D. A., and K. J. Hanson. 1989. Spatial and temporal variability of dust production caused by wind erosion in the United States. *Journal of Geophysical Research* 94 (D2): 2197–206.

Goudie, A. S. 1983. Dust storms in space and time. *Progress in Physical Geography* 7:502–30.

Goudie, A. S., and N. J. Middleton. 1992. The changing frequency of dust storms through time. *Climatic Change* 20:197–225.

Goudie, A. S., and N. J. Middleton. 2001. Saharan dust storms: nature and consequences. *Earth-Science Reviews* 56:179–204.

Goudie, A. S., and G. L. Wells. 1995. The nature, distribution, and formation of pans in arid zones. *Earth-Science Reviews* 38: 1–69.

Grayson, D. K. 1993. *The desert's past: A natural history of the Great Basin*. Washington, DC: Smithsonian Institution Press.

Grigoryev, A. A., and K. J. Kondratyev. 1981. Atmospheric dust observed from space. Part 2. *WMO Bulletin* 30:3–9.

Herman, J. R., P. K. Bhartia, O. Torres, C. Hsu, C. Seftor, and E. Celarier. 1997. Global distribution of UV-absorbing aerosols from Nimbus 7/TOMS data. *Journal of Geophysical Research* 102:16911–22.

Herman, J. R., N. Krotkov, E. Celarier, D. Larko, and G. Labow. 1999. Distribution of UV radiation at the Earth's surface from TOMS-measured UV-backscattered radiances. *Journal of Geophysical Research–Atmospheres* 104 (D10):12059–76.

Holben, B., T. F. Eck, and R. S. Fraser. 1991. Temporal and spatial variability of aerosol optical depth in the Sahel region in relation to vegetation remote sensing. *International Journal of Remote Sensing* 12:1147–63.

Honda, M., and H. Shimuzu. 1998. Geochemical, mineralogical, and sedimentological studies on the Taklimakaan Desert sands. *Sedimentology* 45:1125–43.

Husar, R. B., J. D. Husar, and L. Martin. 2000. Distribution of continental surface aerosol extinction based on visual range data. *Atmospheric Environment* 34 (29–30): 5067–78.

Husar, R. B., J. M. Prospero, and L. L. Stowe. 1997. Characterization of tropospheric aerosols over the oceans with the NOAA advanced very high resolution radiometer optical thickness operational product. *Journal of Geophysical Research–Atmospheres* 102 (D14): 16889–909.

Idso, S. B. 1976. Dust storms. *Scientific American* 235 (4): 108–11, 113–14.

Ing, G. K. T. 1969. A dust storm over central China, April 1969. *Weather* 27:136–45.

Iwasaka, Y., H. Minoura, and K. Nagaya. 1983. The transport and spatial scale of Asian dust-storm clouds: A case study of the dust-storm event of April 1979. *Tellus* 35B:189–96.

Jaffe, D. A., A. Mahura, J. Kelley, J. Atkins, P. C. Novelli, and J. Merrill. 1997. Impact of Asian emissions on the remote North Pacific atmosphere: Interpretation of CO data from Shemya, Guam, Midway and Mauna Loa. *Journal of Geophysical Research* 102 (28): 627–28, 636.

Johnson, A. M. 1976. The climate of Peru, Bolivia, and Ecuador. In *World survey of climatology*, vol. 12, ed. W. Schwerdtfeger, 147–202. Amsterdam: Elsevier Scientific.

Joseph, P. V. 1982. A tentative model of Andhi. *Mausam* 33:417.

Kalnay, E., M. Kanamitsu, R. Kistler, W. Collins, D. Deaven, L. Gandin, M. Iredell, S. Saha, G. White, J. Woollen, Y. Zhu, A. Leetmaa, R. Reynolds, M. Chelliah, W. Ebisuzaki, W. Higgins, J. Janowiak, K. C. Mo, C. Ropelewski, C. J. Wang, R. Jenne, and D. Joseph. 1996. The NCEP/NCAR 40-year reanalysis project. *Bulletin American Meteorological Society* 77:437–71.

Kalu, A. E. 1979. The African dust plume: Its characteristics and propagation across West Africa in winter. In *Sahara dust: Mobilization, transport, deposition*, ed. C. Morales, 95–118. Chichester, U.K.: John Wiley and Sons.

Kes, A. S., and B. A. Fedorovich. 1976. Process of forming aeolian dust in space and time. In *23rd International Geographical Congress* section 1, ed. I. P. Gerasimor, 174–77. Moscow: International Geographical Union.

King, M. D., Y. J. Kaufman, D. Tanre, and T. Nakajima. 1999. Remote sensing of tropospheric aerosols from space: Past, present and future. *Bulletin American Meteorological Society* 80:2229–59.

Klimenko, L. V., and L. A. Moskaleva. 1979. Frequency of occurrence of dust storms in the USSR. *Meteorologiya I Gidrologiya* 9:93–97.

Lavenu, A., M. Fournier, and M. Sebrier. 1984. Existence de nouveaux episodes lacustres quaternaires dans l'Altiplano Peruvo-Bolivien (Existence of new quaternary lake episodes in Peruvian-Bolivian Altiplano). *Orstrom ser Geologie* 14:103–14.

Lee, J. A., B. L. Allen, R. E. Peterson, J. M. Gregory, and K. E. Moffett. 1994. Environmental controls on blowing dust direction at Lubbock, Texas, U.S.A. *Earth Surface Processes and Landforms* 19:437–49.

Legrand, M., J. J. Bertrand, M. Desbois, L. Meneger, and Y. Fouquart. 1989. The potential of satellite infrared satellite data for the retrieval of Saharan dust optical depth over Africa. *Journal of Applied Meteorology* 28:309–18.

Leroy, M., J. L. Deuze, F. M. Breon, O. Hautecoeur, M. Herman, J. C. Buriez, D. Tanre, S. Bouffies, P. Chazette, and J. L. Roujean. 1997. Retrieval of aerosol properties and surface bi-directional reflectances from POLDER/ADEOS. *Journal of Geophysical Research* 102:17023–37.

Littmann, T. 1991. Dust-storm frequency in Asia: Climatic control and variability. *International Journal of Climatology* 11:393–412.

Magee, J. W., and G. H. Miller. 1998. Lake Eyre palaeohydrology from 60 ka to the present: Beach ridges and glacial maximum

aridity. *Palaeogeography, Palaeoclimatology, Palaeoecology* 144 (3–4): 307–29.
Mainguet, M., and M. C. Chemin. 1990. Le Massif du Tibesti dans le système éolien du Sahara: Reflexion sur la génèse du Lac Tchad (The Massif of Tibesti and the wind system of the Sahara: Reflections on the gensisi of Lake Chad). *Berliner Geographische Studien* 30:261–76.
Matson, M., and B. Holben. 1987. Satellite detection of tropical burning in Brazil. *International Journal of Remote Sensing* 8:509–16.
McTainsh, G. H. 1985. Dust processes in Australia and West Africa: A comparison. *Search* 16: 104–6.
McTainsh, G. H., R. Burgess, and J. R. Pitblado. 1989. Aridity, drought, and dust storms in Australia (1960–84). *Journal of Arid Environments* 16:11–22.
Middleton, N. J. 1984. Dust storms in Australia: Frequency, distribution, and seasonality. *Search* 15:46–47.
———. 1985. Effect of drought on dust production in the Sahel. *Nature* 316 (6027): 431–35.
———. 1986a. Dust storms in the Middle East. *Journal of Arid Environments* 10:83–96.
———. 1986b. A geography of dust storms in southwest Asia. *Journal of Climatology* 6:183–96.
———. 1986c. The geography of dust storms. D.Phil. thesis, Department of Geography, University of Oxford.
———. 1991. Dust storms in the Mongolian People's Republic. *Journal of Arid Environments* 20:287–97.
Middleton, N. J., and A. S. Goudie. 2001. Saharan dust: Sources and trajectories. *Transactions of the Institute of British Geographers* NS 26:165–81.
Middleton, N. J., A. S. Goudie, and G. L. Wells. 1986. The frequency and source areas of dust storms. In *Aeolian geomorphology*, ed. W. G. Nickling, 237–59. Boston: Allen and Unwin.
Mo, K. C., and R. W. Higgins. 1996. Large-scale atmospheric moisture transport as evaluated in the NCEP/NCAR and NASA/DAO reanalyses. *Journal of Climate* 9:1531–45.
Mohsin, S. I., M. A. Farooqui, and M. Danish. 1989. A textural study of nearshore recent sediments, Makran coast, Pakistan. *Pakistan Journal of Scientific and Industrial Research* 32 (1): 13–16.
Moulin, C., F. Guillard, F. Dulac, and C. E. Lambert. 1997. Long-term daily monitoring of Saharan dust load over ocean using Meteosat ISCCP-B2 data Part 1: Methodology and preliminary results for 1983–1994 in the Mediterranean. *Journal of Geophysical Research* 102:16947–58.
Nash, D. J., D. S. G. Thomas, and P. A. Shaw. 1994. Timescales, environmental change, and dryland valley development. In *Environmental change in drylands*, ed. A. C. Millington and K. Pye, 25–41. Chichester, U.K.: John Wiley and Sons.
Negi, B. S., S. Sadasivan, K. S. V. Nambi, and B. M. Pande. 1996. Characterization of atmospheric dust at Gurushikar, Mt. Abu, Rajasthan. *Environmental Monitoring and Assessment* 40 (3): 253–59.
Nickling, W. G., G. H. McTainsh, and J. F. Leys. 1999. Dust emissions from the Channel Country of western Queensland, Australia. *Zeitschrift für Geomorphologie Supplementband* 116:1–17.
Orgill, M. M., and G. A. Sehmel. 1976. Frequency and diurnal variation of dust storms in the contiguous U.S.A. *Atmospheric Environment* 10:813–25.
Pease, P. P., V. P. Tchakerian, and N. W. Tindale. 1998. Aerosols over the Arabian Sea: Geochemistry and source areas for aeolian transport. *Journal of Arid Environments* 39:477–96.
Petit-Maire, N., ed. 1991. *Paleoenvironnements du Sahara (Palaeoenvironments of the Sahara)*. Paris: Editions du CNRS.
Prinz, E. M., and W. P. Wenzel. 1992. Geostationary satellite detection of biomass burning in South America. *International Journal of Remote Sensing* 13:2783–99.
Prospero, J. M., and T. N. Carlson. 1981. Saharan air outbreaks over the tropical North Atlantic. *Pure and Applied Geophysics* 119 (3): 677–91.
Prospero, J. M., P. Ginoux, O. Torres, S. E. Nicholson, and T. E. Gill. 2002. Environmental characterization of global sources of atmospheric soil dust identified with the Nimbus-7 Total Ozone Mapping Spectrometer (TOMS) absorbing aerosol product. *Reviews of Geophysics* 40 (4), doi: 10.1029/2000RG000095.
Prospero, J. M., and D. L. Savoie. 1989. Effect of continental sources of nitrate concentrations over the Pacific Ocean. *Nature* 339:687–89.
Reheis, M. 1997. Dust deposition of Owens (dry) Lake, 1991–1994: Preliminary findings. *Journal of Geophysical Research* 102:25999–6008.
Reheis, M., and R. Kihl. 1995. Dust deposition in southern Nevada and California, 1984–1989: Relations to climate, source area, and source lithology. *Journal of Geophysical Research* 100 (D5): 8893–918.
Reyss, J. L., P. A. Pirazzoli, A. Haghipour, C. Hatte, and M. Fontugne. 1998. Quaternary marine terraces and tectonic uplift rates on the south coast of Iran. *Geological Society Special Publication* 146:225–37.
Rosenfield, J. E., D. B. Considine, P. E. Meade, J. T. Bacmeister, C. H. Jackman, and M. R. Schoeberl. 1997. Stratospheric effects of Mount Pinatubo aerosol studied with a coupled two-dimensional model. *Journal of Geophysical Research* 102 (D3): 3649–70.
Rouchy, J. M., M. Servant, M. Fournier, and C. Causse. 1996. Extensive carbonate algal bioherms in upper Pleistocene saline lakes of the central Altiplano of Bolivia. *Sedimentology* 43:973–93.
Schutz, L., R. Jaenicke, and H. Pietrek. 1981. Saharan dust transport over the North Atlantic Ocean (Geological Society of American Special Paper 186). In *Desert dust: Origin, characteristic, and effect on man*, ed. T. L. Pewe, 87–100. Boulder, CO: Geological Society of America.
Schwartz, S. E., R. Wagener, and S. Nemesure. 1995. Microphysical and compositional influences on shortwave radiative forcing of climate by sulfate aerosols. *Abstracts of Papers of the American Chemical Society* 209: 2-ENVR Part 1.
Sirocko, F. 1991. Deep-sea sediments of the Arabian Sea: A paleoclimatic record of the southwest-Asian summer monsoon. *Geologische Rundschau* 80:557–66.
Sprigg, R. C. 1982. Alternating wind cycles of the Quaternary era and their influence on aeolian sedimentation in and around the dune deserts of south-eastern Australia. In *Quaternary dust mantles of China, New Zealand, and Australia*, ed. R. J. Wasson, 211–40. Proceedings of workshop at the Australian National University, Canberra, 3–5 December 1980. Canberra, Australia: Australian National University Press.
Sturman, A., and N. Tapper. 1996. *The weather and climate of Australia and New Zealand*. Oxford: Oxford University Press.
Svensson, A., P. E. Biscaye, and F. E. Grousset. 2000. Characterization of late glacial continental dust in the Greenland Ice Core Project ice core. *Journal of Geophysical Research* 105 (D4): 4637–56.

Swap, R., M. Garstang, and S. Greco. 1992. *Saharan dust in the Amazon Basin*. *Tellus* B44 (2): 133–49.

Talbot, R. W., J. E. Dibb, B. L. Lefer, J. D. Bradshaw, S. T. Sandholm, D. R. Blake, N. J. Blake, G. W. Sachse, J. E. Collins, B. G. Heikes, J. T. Merrill, G. L. Gregory, B. E. Anderson, H. B. Singh, D. C. Thornton, A. R. Bandy, and R. F. Pueschel. 1997. Chemical characteristics of continental outflow from Asia to the troposphere over the western Pacific Ocean during February–March 1994: Results from PEM-West B. *Journal of Geophysical Research* 102: 28,255–74.

Tegen, I., D. Koch, A. A. Lacis, and M. L. Sato. 2000. Trends in tropospheric aerosol loads and corresponding impact on direct radiative forcing between 1950 and 1990: A model study. *Journal of Geophysical Research–Atmospheres* 105 (D22): 26,971–89.

Tegen, I., A. A. Lacis, and I. Fung. 1996. The influence on climate forcing of mineral aerosols from disturbed soils. *Nature* 380 (6573): 419–22.

Thomas, D. S. G., and P. Shaw. 1991. *The Kalahari environment*. Cambridge, U.K.: Cambridge University Press.

Tindale, N. W., and P. P. Pease. 1999. Aerosols over the Arabian Sea: Atmospheric transport pathways and concentrations of dust and sea salt. *Deep-Sea Research Part II* 46:1577–95.

Todhunter, P. E., and L. J. Cihacek. 1999. Historical reduction of airborne dust in the Red River Valley of the North. *Journal of Soil and Water Conservation* 54:543–51.

Torres, O., P. K. Bhartia, J. R. Herman, Z. Ahmad, and J. Gleason. 1998. Derivation of aerosol properties from satellite measurements of backscattered ultraviolet radiation: Theoretical basis. *Journal of Geophysical Research* 103:17099–110.

Tyson, P. D., and R. A. Preston-Whyte. 2000. *The atmosphere, weather, and climate of southern Africa*. Cape Town: Oxford University Press.

Urvoy, Y. 1942. Les basins du Niger (Basins of Niger). *Mémoires de l'Institut Fondamental d'Afrique Noire*, vol. 4.

Vita-Finzi, C. 1981. Late Quaternary deformation on the Makran coast of Iran. *Zeitschrift für Geomorphologie, Supplementband* 40:213–26.

Wang, T., and G. Dong. 1994. Sand sea history of the Taklimakan for the past 30,000 years. *Geografiska Annaler* 76A:131–41.

Wasson, R. J., K. Fitchett, B. Mackey, and R. Hyde. 1988. Large-scale patterns of dune type, spacing, and orientation in the Australian continental dunefield. *Australian Geographer* 19:89–104.

Wellington, J. H. 1938. The Kunene River and the Etosha Plain. *South African Geographical Journal* 20:21–32.

White, B. R. 1979. Soil transport by wind on Mars. *Journal of Geophysical Research* 84:4643–51.

Wigner, K. A., and R. E. Peterson. 1987. Synoptic climatologies of blowing dust on the Texas South Plains, 1947–1984. *Journal of Arid Environments* 13:199–209.

Willis, D. M., M. G. Easterbrook, and F. R. Stephenson. 1980. Seasonal variation of oriental sunspot sightings. *Nature* 287:617–19.

Wilshire, H. G., J. K. Nakata, and B. Hallet. 1981. Field observations of the December 1977 wind storm, San Joaquin Valley, California. In *Desert dust: Origins, characteristics, and effects on man*, ed. T. L. Péwé, 233–51. Boulder, CO: Geological Society of America.

Worster, D. 1979. *Dust Bowl: The Southern Plains in the 1930s*. New York: Oxford University Press.

Xuan, J., L. Gualiang, and K. Du. 2000. Dust emission inventory in Northern China. *Atmospheric Environment* 34:4565–70.

Zaizen, Y., M. Ikegami, K. Okada, and Y. Makino. 1995. Aerosol concentration observed at Zhangye in China. *Journal of the Meteorological Society of Japan* 73:891–97.

Zhang, X. Y., R. Arimoto, and Z. S. An. 1997. Dust emission from Chinese desert sources linked to variations in atmospheric circulation. *Journal of Geophysical Research* 102 (D23): 28041–47.

Zhang, X. Y., R. Arimoto, G. H. Zhu, T. Chen, and G. Y. Zhang. 1998. Concentration, size-distribution, and deposition of mineral aerosol over Chinese desert regions. *Tellus* 50B: 317–30.

Zhu, Z. 1984. Aeolian landforms in the Taklimakan Desert. In *Deserts and arid lands*, ed. F. El-Baz, 133–44. The Hague: Nijhoff.

Correspondence: School of Geography and the Environment, University of Oxford, Oxford OX1 3TB, U.K., e-mail: richard.washington@geography.ox.ac.uk (Washington); Department of Geography, University College London, London WC1H 0AP, U.K., e-mail: m.todd@ucl.ac.uk (Todd); School of Geography and the Environment, University of Oxford, Oxford OX1 3TB, U.K., e-mail: nicholas.middleton@geog.ox.ac.uk (Middleton); School of Geography and the Environment, University of Oxford, Oxford OX1 3TB, U.K., e-mail: andrew.goudie@geog.ox.ac.uk (Goudie).